Journal of Ceramic Processing Research. Vol. 16, No. 1, pp. 54~58 (2015)

J O U R N A L O F
Ceramic Processing Research

Synthesis and characterization of paramagnetic Mn doped $Ca_2P_2O_7$ ceramics by sol-gel method

Omer Kaygili*
Department of Physics, Faculty of Science, Firat University, 23119 Elazig, Turkey

Pure calcium pyrophosphate ($Ca_2P_2O_7$) and Mn doped $Ca_2P_2O_7$ based ceramics were synthesized by sol–gel method, and were characterized using X-ray diffraction (XRD), Fourier transform infrared (FTIR), vibrating sample magnetometer (VSM), scanning electron microscopy (SEM) and energy dispersive X-ray (EDX) spectroscopy. The average crystallite size and crystallinity are affected by the addition of lower amount Mn, whereas, the content of Mn having higher amounts did not cause a remarkable effect on these parameters. The bands belonging to the pyrophosphates were detected. The ceramics exhibit the paramagnetic behavior at room temperature and the magnetic susceptibility increases from 7.28×10^{-7} to 2.48×10^{-5} emu g^{-1} Oe^{-1} with the addition of Mn. The microstructure of the ceramics is affected by the content of Mn. All the samples are composed of the fine-grained particles, and no impurity is observed.

Key words: Magnetic property, Sol-gel method, $Ca_2P_2O_7$ ceramic.

Introduction

The demand for magnetic nanoparticles has increased day by day and these materials have been extremely used in medical fields such as anticancer drug delivery, cell label and separation, immunoassay, hyperthermia and magnetic resonant imaging (MRI) [1-5]. Ceramics are preferred in the biotechnological applications, since the production of nano-structured and non-toxic materials is gained a great importance [6, 7]. $Ca_2P_2O_7$ compound is one of the most preferable ceramics used as biomaterial, as well as the best known calcium phosphates including hydroxyapatite (HAp), tricalcium phosphate (TCP) and tetracalcium phosphate (TTCP) [8-11].

Manganese (Mn) is a transition metal and, both Mn and its common ions are paramagnetic [12, 13]. Paramagnetic metals have been used as contrast materials for magnetic resonance (MR) since they shorten the longitudinal relaxation time and thus increase the relaxation rate of solvent water protons. Another desired property for MRI is a high-spin number. In this connection, Mn has the desired properties for MRI contrast agent such as a high-spin number; long electronic relaxation time and labile water exchange [14-17]. Mn has a special importance in the central nervous system (CNS). Mn^{2+} can substitute for Ca^{2+} and/or Mg^{2+} because its ionic radius is smaller than both. It has been commonly used in biological and medical applications for decades since Mn^{2+} ions increase the ligand binding affinity of integrin and activate cell adhesion [18-20]. Sopyan *et al*. [21] reported that Mn doping improves the mechanical properties (e.g., the maximum hardness and fracture toughness) of biphasic calcium phosphate ceramics. Braccci *et al*. [22] reported that the relatively high content of Mn^{2+} in the calcium phosphate coating has an exceptional beneficial effect on osteocalcin production, and this effect is much more than that of Sr^{2+}. Huang *et al*. [23] reported that the addition of Mn into HAp improves the *in vitro* biocompatibility of the HAp films.

In this work, the addition of Mn into the non-toxic $Ca_2P_2O_7$ ceramics was chosen to prepare the paramagnetic $Ca_2P_2O_7$ ceramics. As well-known, the magnetic particles are moved from one place to another place by an external magnetic field. The magnetic nanoparticles can be bond a drug, protein, enzyme, antibody or nucleotide and used to move these to the desired location such as an organ, tissue or tumor. In this regard, improving and controlling of the magnetic properties of the biomaterials becomes the more important prerequisite for a biofunctional and target delivery material [24].

This paper presents a detailed investigation report concerning the effects of Mn addition on the crystal structure, chemical, microstructure and magnetic properties of $Ca_2P_2O_7$ nanoceramics by sol-gel method, which is very suitable for the preparation of nanomaterials with high purity and low cost. These properties were characterized by X-ray diffraction (XRD), Fourier transform infrared (FTIR), vibrating sample magnetometry (VSM), scanning electron microscopy (SEM) and energy dispersive X-ray (EDX) spectroscopy.

*Corresponding author:
Tel : +90-424-2370000 / 3623
Fax: +90-424-2330062
E-mail: okaygili@firat.edu.tr

Materials and Method

The samples were synthesized using the sol-gel method, and the experimental processes were summarized as following steps: The Ca/P and (Ca + Mn)/P molar ratios were chosen as the value of 1.67 for Mn-free $Ca_2P_2O_7$ and Mn-assisted $Ca_2P_2O_7$ samples. The samples with 0, 4, 10 and 20 at.% Mn contents were named as M0, M1, M2 and M3, respectively. The moles of all the samples are given in Table 1. Calcium nitrate tetrahydrate ($Ca(NO_3)_2 \cdot 4H_2O$), phosphorus pentoxide (P_2O_5) and manganese (II) nitrate tetrahydrate ($Mn(NO_3)_2 \cdot 4H_2O$) were purchased from Merck and used without any purification. These chemicals were separately dissolved in anhydrous ethanol (C_2H_5OH, Sigma-Aldrich) using a magnetic stirrer. A solution of P_2O_5 was added drop-wise into a solution of $Ca(NO_3)_2 \cdot 4H_2O$ under rapid stirring at 20 ºC, and a solution of $Mn(NO_3)_2 \cdot 4H_2O$ was added drop-wise into this solution. Then, the new solution was stirred vigorously for 30 min. The dissolved solution was mixed in the ultrasonic bath for 10 min. The pH was adjusted the value of 10 by adding of ammonium hydroxide (NH_4OH, Sigma-Aldrich) and the solution was centrifuged at 4000 rpm for 5 min. Then, this precipitate was filtered and washed two times. This was dried at 100 ºC for 3 h and heated at 700 ºC for 2 h. While a white powder was obtained for M0, the three powders having the different shades of light pink color were obtained for M1, M2 and M3.

X-ray diffraction (XRD) analyses were performed on a Bruker D8 Advance diffractometer operated at 40 kV and 40 mA. Fourier transform infrared (FTIR) spectra were collected by a PerkinElmer Spectrum One spectrophotometer in the range of 400-4000 cm^{-1}. The investigation of the morphology and elemental compositions of the samples was carried out using a scanning electron microscope (SEM, ZEISS EVO 50) equipped with an energy dispersive X-ray (EDX, Oxford Instruments Inca Energy 350) spectrometer operated at 10 kV. Magnetic properties were studied by a vibrating sample magnetometer (VSM) in the magnetic field interval of –90,000 and 90,000 Oe.

Results and Discussion

Fig. 1 shows the XRD patterns of Mn-free and Mn-doped ceramic samples. The major phase for all the samples is identified as $Ca_2P_2O_7$ (PDF No: 9-345) with orthorhombic crystal structure. Furthermore, the minor phase observed for all the Mn-assisted samples is determined as $CaMnP_2O_7$ (PDF No: 85-1938) with triclinic crystal structure. Mn-addition in calcium pyrophosphate structure causes the formation of a new mixing manganese calcium phosphate phase and this result is in agreement with Masala *et al*. [25].

The average crystallite size, *D*, of the samples can be calculated according to the following Scherrer formula [26]:

$$D = \frac{0.9\lambda}{B_{1/2}cos\theta} \quad (1)$$

where λ is the wavelength of the X-rays (λ = 0.15406 nm for CuKα radiation), $B_{1/2}$ is the full width at half maximum (FWHM) in radian and θ is the diffraction angle in degree. The calculated values of the average crystallite size were found to be 21.45, 24.48, 26.12 and 25.96 nm for M0, M1, M2 and M3, respectively. The average crystallite size of undoped sample is smaller than those of Mn-containing samples. The crystallinity was calculated according to the previous work [27], and it was found to be 72, 65, 64 and 65% for M0, M1, M2 and M3, respectively. The crystallinity of Mn-free sample is higher than those of Mn-containing ones. It is clearly seemed that the small amounts of Mn affect the crystallinity and this result is in perfect harmony with the Masala *et al*. [25]. The amount of Mn, ranging from 4 to 20 at.%, in calcium pyrophosphate structure has not a dramatic effect on the average crystallite size and crystallinity if we make a comparison among Mn-doped samples.

FTIR spectra of all the samples are shown in Fig. 2. The bands belonging to the different vibrational modes of the phosphate groups were observed at 505, 559, 576, 601, 983 and 1027 cm^{-1}. Additionally, the other peaks detected at 753, 1117 and 1160 cm^{-1} are attributed to the stretching modes of $P_2O_7^{4-}$ [28]. These findings support the pyrophosphate based phases identified on the XRD. The bands at 1632 and 3431 cm^{-1} are

Table 1. The moles of the as–synthesized samples.

Sample	$Ca(NO_3)_2 \cdot 4H_2O$ (mol)	$Mn(NO_3)_2 \cdot 4H_2O$ (mol)	P_2O_5 (mol)
M0	0.050	–	0.015
M1	0.048	0.002	0.015
M2	0.045	0.005	0.015
M3	0.040	0.010	0.015

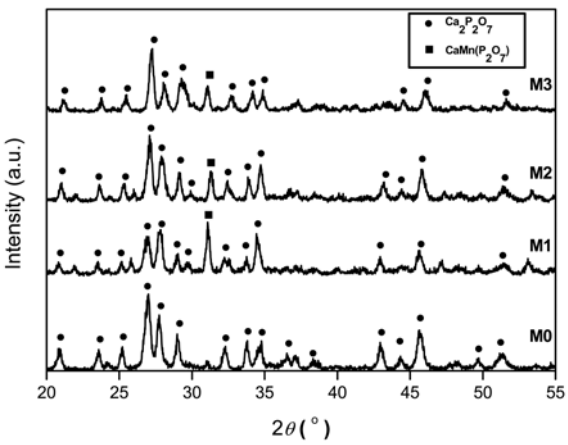

Fig. 1. XRD patterns of the samples.

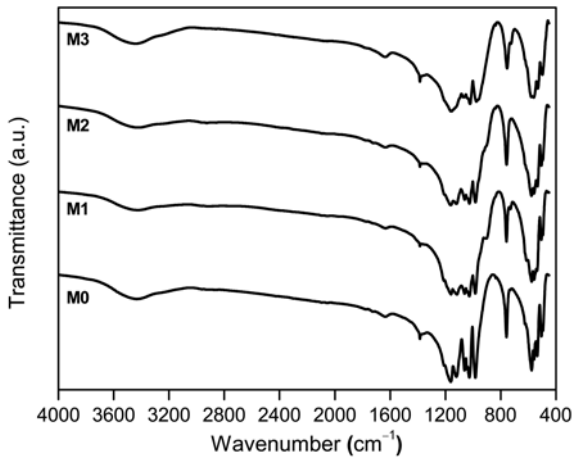

Fig. 2. FTIR spectra of the samples.

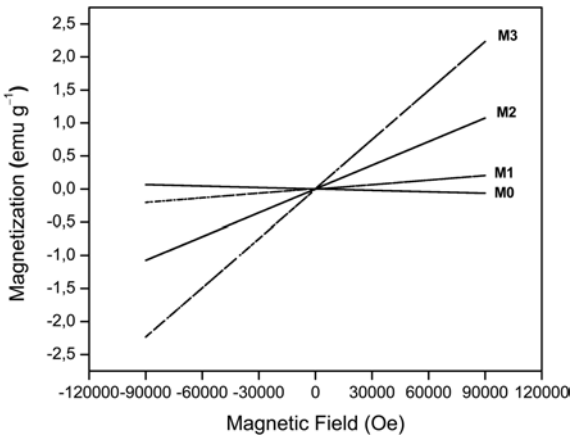

Fig. 3. Magnetization vs. magnetic field curves of the samples at room temperature.

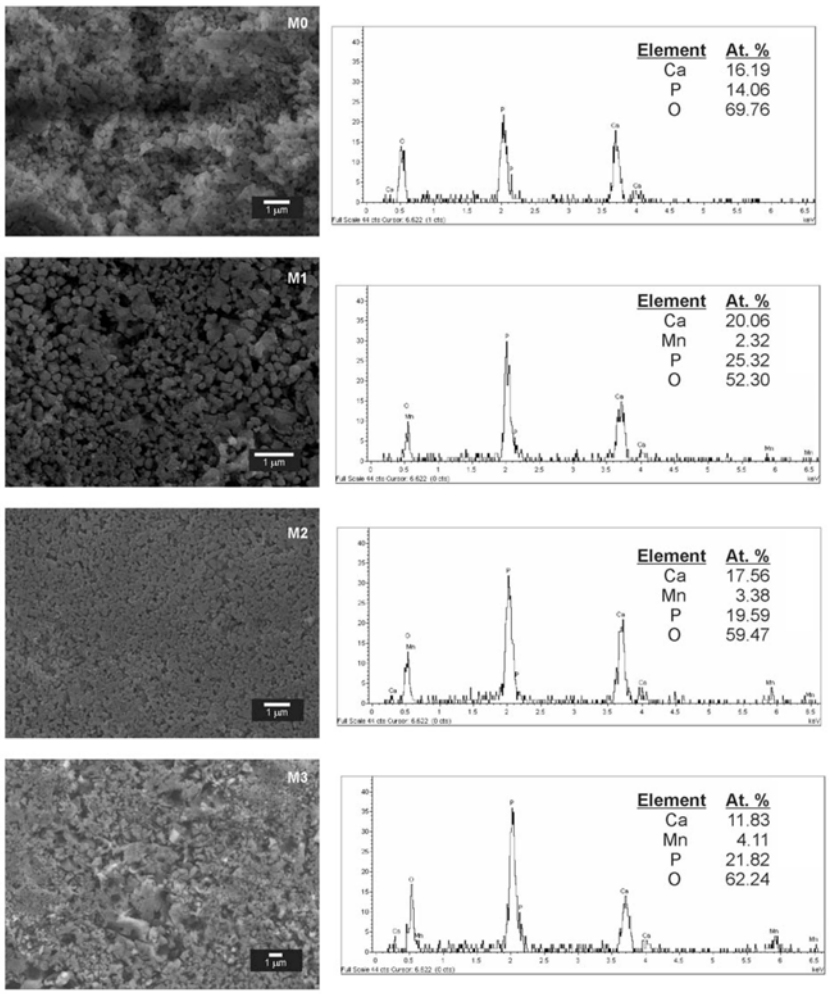

Fig. 4. SEM images and EDX results of the samples.

assigned to the adsorbed water. The band originated from the nitrates was detected at 1383 cm^{-1} [27].

Fig. 3 shows the magnetization vs. field graphs of the samples. The change of the magnetization with field is linear, and it does not observe any hysteresis curve. The linearity in magnetization curves confirms that the synthesized samples exhibit the paramagnetic behavior at room temperature [29, 30]. The magnetization increases with increasing magnetic field. The maximum values of the magnetization at 90,000 Oe were found to be 0.06, 0.20, 1.07 and 2.23 emu g^{-1} for M0, M1, M2 and M3, respectively. Moreover, the magnetization increases

with the addition of Mn.

For paramagnetic behavior, the magnetic susceptibility (χ) is calculated using the following equation [31, 32]

$$\chi = \frac{M}{H} \quad (2)$$

where M is the magnetization of the sample and H is the magnetic field strength. The obtained values of the magnetic susceptibility were found to be 7.28×10^{-7}, 2.23×10^{-6}, 1.20×10^{-5} and 2.48×10^{-5} emu g^{-1} Oe^{-1} for M0, M1, M2 and M3, respectively. The magnetic susceptibility increases significantly with increasing amount of Mn. The obtained χ values are typical values for the paramagnetic materials.

SEM images and EDX analysis results of the samples are given in Fig. 4. All the samples are composed of the fine-grained particles, which are usually smaller than 1 μm. The microstructure shows a change with the amount of Mn. Namely, the distribution of the particles is almost uniform for M0, M1 and M2, whereas at higher Mn content (M3) non-uniform particle distribution is observed. Ca, P, O and Mn were detected from the EDX analyses, and no impurity was observed. It is seen that the amount of Ca decreases, while the amount P increases. As expected, Mn content detected from EDX for samples M1, M2 and M3 increases with increasing amount of Mn. The Ca/P ratio of M0 was found to be 1.15. The (Ca + Mn)/P ratios of M1, M2 and M3 were found to be 0.88, 1.07 and 0.73, respectively. The decrease in (Ca + Mn)/P ratios indicates the Ca-deficiency. The theoretical values of Mn/Ca ratio during the synthesis were adjusted to 0.087, 0.250 and 0.667 for M1, M2 and M3, respectively. Their experimental values are respectively found to be 0.120, 0.192 and 0.347. This result means that the ion exchange between Ca^{2+} and Mn^{2+} increases with the increase of Mn, but this increase is less than theoretical expected values. Furthermore, the EDX results indicate that Mn is not homogeneously distributed over the samples and this is in agreement with the result reported by Mayer *et al*. [19].

Conclusions

Pure– and Mn-containing $Ca_2P_2O_7$ ceramics were successfully synthesized via the sol-gel route. From the XRD results, the addition of Mn in $Ca_2P_2O_7$ ceramic having the orthorhombic crystal structure causes the formation of the secondary phase ($CaMnP_2O_7$) with the triclinic crystal structure. Although, the average crystallite size and crystallinity are affected by the addition of Mn at the lower amount, the amount of Mn at higher amounts does not cause a remarkable effect on these parameters. The vibration modes of pyrophosphate groups were detected from the FTIR spectra, and this verifies the phases belonging to calcium pyrophosphates in the XRD patterns. The magnetization increases with increasing magnetic field. Furthermore, the magnetization increases when the amount of Mn is increased. The maximum values of the magnetization at 90,000 Oe are in the range of 0.06-2.23 emu g^{-1}. The magnetic susceptibility increases from 7.28×10^{-7} to 2.48×10^{-5} emu g^{-1} Oe^{-1} with increasing amount of Mn. From the SEM observations, it is seen that all the samples are composed of the fine-grained particles. The microstructure shows a change with the amount of Mn. Consequently, the above-mentioned properties of $Ca_2P_2O_7$ nanoceramics can be controlled by the Mn dopant.

Acknowledgments

This work was supported by Management Unit of Scientific Research projects of Firat University (FÜBAP) (Project Number: FF.12.31).

References

1. R.K. Singh, A.M. El-Fiqi, K.D. Patel, and H.W. Kim, Mater. Lett. 75 (2012) 130-133.
2. Y. Yamada, K.I. Kurumada, K. Susa, N. Umeda, and G. Pan, Adv Powder Technol. 18 [3] (2007) 251-260.
3. A.A.M. Elsherbini, M. Saber, M. Aggag, A. El-Shahawy, and H.A.A. Shokier, Magn. Reson. Imaging 29 [2] (2011) 272-280.
4. C.H. Hou, S.M. Hou, Y.S. Hsueh, J. Lin, H.C. Wu, and F.H. Lin, Biomaterials 30 [23-24] (2009) 3956-3960.
5. D. Gopi, M.T. Ansari, E. Shinyjoy, and L. Kavitha, Spectrochim. Acta Part A 87 (2012) 245-250.
6. O. Kaygili, S. Keser, T. Ates, and F. Yakuphanoglu, Ceram. Int. 39 [7] (2013) 7779-7785.
7. I. Sopyan, and A.N. Natasha, Ionics 15 [6] (2009) 735-741.
8. D. Shi, "Introduction to Biomaterials"(Tsinghua University Press and World Scientific Publishing Co. Pte. Ltd., 2006).
9. J. Park, "Bioceramics: Properties, Characterizations, and Applications"(Springer, 2008).
10. J.J. Bian, D.W. Kim, and K.S. Hong, Mater. Lett. 58 [3-4] (2004) 347-351.
11. F.H. Lin, J.R. Liaw, M.H. Hon, and C.Y. Wang, Mater. Chem. Phys. 41 [2] (1995) 110-116.
12. M. Halka, and B. Nordstrom, "Periodic Table of the Elements: Transition Metals" (Oxford University Press, 2011).
13. D.R. Lide, "CRC Handbook of Chemistry and Physics" (CRC Press,2002).
14. M. Schaefer, Met. Based Drugs 4 [3] (1997) 159-171.
15. D. Pan, A.H. Schmieder, S.A. Wickline, and G.M. Lanza, Tetrahedron 67 [44] (2011) 8431-8444.
16. S. Aime, P. Anelli, M. Botta, M. Brocchetta, S. Canton, F. Fedeli, E. Gianolio, and E. Terreno, J. Biol. Inorg. Chem. 7 [1-2] (2002) 58-67.
17. D. Pan, S.D. Caruthers, A. Senpan, A.H. Schmieder, S.A. Wickline, and G.M. Lanza, Wiley Interdiscip. Rev. Nanomed. Nanobiotechnol. 3 [2] (2011) 162-173.
18. T.E. Gunter, J.S. Puskin, and P.R. Russell, Biophys. J. 15 [4] (1975) 319-333.
19. I. Mayer, O. Jacobsohn, T. Niazov, J. Werckmann, M. Iliescu, M. Richard-Plouet, O. Burghaus, and D. Reinen, Eur. J. Inorg. Chem. 7 (2003) 1445-1451.

20. Y. Li, J. Widodo, S. Lim, and C.P. Ooi, J. Mater. Sci. 47 [2] (2012) 754-763.
21. I. Sopyan, N.A. Nawawi, Q.H. Shah, S. Ramesh, C.Y. Tan, and M. Hamdi, Mater. Manuf. Processes 26 [7] (2011) 908-914.
22. B. Bracci, P. Toricelli, S. Panzavolta, E. Boanini, R. Giardino, and A. Bigi, J. Inorg. Biochem. 103 [12] (2009) 1666-1674.
23. Y. Huang, Q. Ding, S. Han, Y. Yan, and X. Pang, J. Mater. Sci.: Mater. Med. 24 [8] (2013) 1853-1864.
24. S. Laurent, D. Forge, M. Port, A. Roch, C. Robic, L. Vander Elst, and R.N. Muller, Chem. Rev. 108 (2008) 2064-2110.
25. O. Masala, E.J.L. McInnes, and P. O'Brien, Inorg. Chim. Acta 339 (2002) 366-372.
26. B.D. Cullity, "Elements of X-ray diffraction"(Addison-Wesley Publishing Company, 1978).
27. O. Kaygili, S. Keser, T. Ates, A.A. Al-Ghamdi, and F. Yakuphanoglu, Powder Technol. 245 (2013) 1-6.
28. K. Elkabouss, M. Kacimi, M. Ziyad, S. Ammar, and F. Bozon-Verduraz, J. Catal. 226 [1] (2004) 16-24.
29. T.R. Bastami, and M.H. Entezari, Ultrason. Sonochem. 19 [4] (2012) 830-840.
30. P. Brandão, J. Rocha, M.S. Reis, A.M. dos Santos, and R. Jin, J. Solid. State Chem. 182 [2] (2009) 253-258.
31. L. Valenzuela, "Magnetic Ceramics" (Cambridge University Press, 1994).
32. H.W. Xu, J. Iwasaki, T. Shimizu, H. Satoh, and N. Kamegashira, J. Alloy Compd. 221 [1-2] (1995) 274-279.